



Research articles

Undistorted 180° phase reversal of magnetoelectric coupling in bi-layered multiferroic laminate

Jitao Zhang^{a,*}, Kang Li^a, Dongyu Chen^a, D.A. Filippov^b, Qingfang Zhang^a, Jie Wu^a, Jiagui Tao^c, Lingzhi Cao^{a,*}, Gopalan Srinivasan^d

^a College of Electrical and Information Engineering, Zhengzhou University of Light Industry, Zhengzhou 450002, China

^b Institute of Electronic and Information Systems, Novgorod State University, Veliky Novgorod 173003, Russia

^c State Grid of Jiangsu Electric Power Co., Ltd., Nanjing 210024, China

^d Physics Department, Oakland University, Rochester, MI 48309, USA

A B S T R A C T

A methodology of rotating the applied static magnetic field on Ni_{0.8}Zn_{0.2}Fe₂O₄ (NZFO)/PZT-8 magnetoelectric laminate, was introduced to realize 180° phase reversal with constant amplitude, which is invariably required for phase-based communication system, engineering technology and microelectronic devices. Through further decoding the phase information existed in magnetoelectric coefficient, we found that the undistorted 180° phase reversal can be achieved once the applied field was reversed. Moreover, piezomagnetic response can essentially track the magnetoelectric response under optimum bias with the variations of rotation angle, and then the origins can be well explained. Experimental results show that the maximum resonance ME voltage coefficient of +51.72 V/cm Oe and −51.93 V/cm Oe were obtained in angle of $\theta = 0^\circ$ and 180°, respectively. These results provide great possibilities for practical applications in ME phase shifters and inverters.

1. Introduction

Magnetoelectric (ME) materials in composite of magnetostrictive and piezoelectric subsystems have received considerable interests due to their great promising applications in multifunctional microelectronic devices [1–4]. From historical perspective, the development of ME materials began from the earliest 1980s in ‘natural’ single-phase compounds to the nearest vivid ‘artificial’ ME heterostructures with various polarized/magnetized schemes and materials combination. Recently the major objective in this invigorated research field is devoted to further enhancing the ME couplings, revealing its underlying physics and exploring novel multifunctional electronic devices [5–10]. In general, the ME effects can be aroused by subjecting the sample to AC magnetic field (H_{AC}) with superimposed applied DC magnetic field (H_{DC}). In this case, the ME couplings undergoes a dynamic magneto-mechanical-electric conversion through mediated strain, change, exchange bias, spin torque *etc* [11–14]. Previously the ME voltage coefficient (α) was employed to characterize the coupling strength quantitatively, while the phase is only considered as supplemental data [15,16]. In fact, the generated ME voltage from piezoelectric layer was triggered by an AC magnetic field [17,18]. In light of this, complex quantity form of α can be given as $\alpha = |\alpha|e^{i\varphi} = |\alpha|\cos(\varphi) - i|\alpha|\sin(\varphi)$ ($\varphi = \alpha' - i\alpha''$ (α' and α'' represent its real and imaginary parts, while $|\alpha|$ and φ are the amplitude and phase angle, respectively) [19,20]. For

practical applications, focused efforts are essential on its amplitude to characterize the field detection sensitivity in ME magnetic sensors [21–23], while the phase angle serving as another principal parameter can provide more valuable information compared with amplitude especially in harsh environment with extremely low signal-to-noise ratio [24]. For instance, in 2008 Liu et al. reported a ME magnetic sensor utilizing phase shifting of electric-field-induced magnetization effects for weak H_{DC} detection, and the achievable sensitivity limit for H_{DC} reaches as low as 10^{-9} T [25]. In 2015, Zhang et al. developed a high-resolution current sensor consisting of ME laminate and high-permeability flux concentrator, phase in the output can be utilized for low-frequency current detection with facilitation of closed magnetic loop and high-sensitivity ME cell [26]. In addition to the extraction of phase signal for magnetic/current detection purposes, the 180° phase shifting (reversal) effect is another major concern. Recently, several experimental researches have dealt with 180° phase shift (reversal) phenomenon in layered ME composite. In 2013, Shi et al. reported magnetic-field-induced 180° phase shift effects in Terfenol-D/PZT bi-layer composite, 180° phase shift around resonance frequency can be achieved by changing H_{DC} from 0.1 T to 0.3 T, accompanying approximately 8 V/A variations in amplitude [27,28]. Subsequently, in 2016 Yang et al. reported the phase shifting effects in circular and rectangle ME composite with PZT/Terfenol-D for comparison studies, and results showed that the appearing 180° phase shifts in circular ME

* Corresponding authors.

E-mail addresses: zhangjitao@zzuli.edu.cn (J. Zhang), lz_cao@outlook.com (L. Cao).

<https://doi.org/10.1016/j.jmmm.2019.165802>

Received 2 June 2019; Received in revised form 30 August 2019; Accepted 5 September 2019

Available online 07 September 2019

0304-8853/ © 2019 Elsevier B.V. All rights reserved.

composite with greater distinct variations of amplitude [29]. In addition, very recently in 2017, the 180° phase reversal effects at resonance frequency were observed in ME laminates with bi-domain 127° Y-cut LiNbO₃ single crystals, but the maximum variable amplitude of ME voltage coefficient reaches 100 V/cm Oe [20]. The process of 180° phase shift (reversal) always accompanies amplitude variations, however, the undesired amplitude variations will lead to a distorted output signal. Therefore, achieving undistorted 180° phase reversal in ME response is compelling for potential applications in phase shifter/inverters

In this study, an effective methodology is introduced to fulfill the requirements of 180° phase reversal with constant amplitude of ME output in bi-layer ferrite/piezoelectric ME laminates, and we try to reveal its origins through investigating the dynamic strain characteristics under applied H_{DC} directions varied from 0° to 360°. To accomplish this goal, controlling the H_{DC} orientations is carried out to activate the complex ME responses, anticipating the 180° phase reversal with constant amplitude of ME response realization in this process. In addition, the H_{DC} orientation induced dynamic piezomagnetic effect in ferrites can account for this as expected. These results provide developments in this field to offer great possibilities in practical use for 180° ME phase shifters and inverters.

2. Experiments

We synthesized polycrystalline nickel zinc ferrite with composition of Ni_{0.8}Zn_{0.2}Fe₂O₄ (NZFO) from starting powders of Fe₂O₃, NiO and ZnO in compliance with its mole ratio through conventional solid-phase sintering methods, which detailed in our previously reported literatures [15]. The sintered bulk NZFO block was cut into thin pieces with dimensions of 23 mm × 5 mm × 0.5 mm. The NZFO slab and piezoelectric ceramic of PZT-8 slab (purchased from Bailing Electronic Ceramics Co., Ltd. Zibo, China) with dimensions of 25 mm × 5 mm × 0.5 mm were bonding together using epoxy adhesive. The sample centered in the solenoid and its longitudinal direction is in parallel with the AC magnetic field (H_{AC}). An optimum DC magnetic field ($H_{DC} = 46$ Oe) was provided by a pair of toroidal permanent magnets (NdFeB N50®, its radius and thickness are 55 mm and 30 mm, respectively), which were mounted on a rotatable fixture with the constant distance of 280 mm, and the solenoid was placed in the center of toroidal permanent magnets. The magnetic field was monitored by gaussmeter at off-resonance and resonance frequencies. The H_{AC} was superimposed with DC magnetic field direction in parallel at initial states, and the 180° phase shift effect can be activated by H_{DC} rotation with angle of θ through adjusting the rotatable fixture. Subsequently, wherein the generated H_{AC} from solenoid was powered by an internal oscillator a lock-in amplifier (Ametek Model SR7280) and the induced ME output across the sample was monitored by the lock-in amplifier. The schematic diagram for measurements was outlined in Fig. 1, dynamic magneto-mechanical responses were characterized by an optical non-contact measurement system with laser Doppler vibrometer (Polytec Model OFV-5000/505). The impedance spectra were measured by an impedance analyzer (Keysight Model E4990A).

3. Results and discussion

Previous experimental and modeling efforts provide clear evidence that the phase shifting effects can be achieved by controlling the magnetic/electric field in ME laminates [25,27,29]. To obtain 180° phase reversal with constant amplitude in ME response, the amplitude ($|\alpha|$) and phase angle (φ) in ME voltage coefficient for bi-layered PZT-8/NZFO laminate were investigated with θ from 0° to 360°. Fig. 2(a) illustrates $|\alpha|_r$ vs θ profiles in polar coordinate under optimum bias of 46 Oe and resonance frequency of $f_r = 84.5$ kHz. As θ is increased from 0° to 90°, $|\alpha|_r$ shows a slight decrease, with θ further increasing, $|\alpha|_r$ undergoes a repetitive response with the increment of 90° alternately

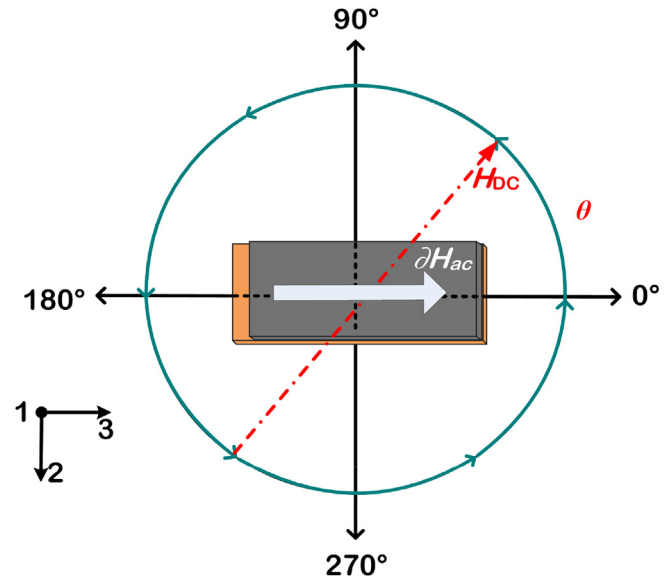


Fig. 1. Schematic diagram of DC field rotations for PZT-8/NZFO composite.

and successively. It is noteworthy that $|\alpha|_r$ exhibits a twofold symmetrical loop in the polar coordinates due to the magnetization and demagnetization effect of the magnetostrictive phase under a variety of θ , similar observations can be found in previous studies [30–32]. This result demonstrated that the constant amplitude of ME response can be achieved by changing the direction of applied H_{DC} . Several representative data including $|\alpha|_r$ vs f and φ vs f profiles around resonance at $\theta = 0^\circ, 90^\circ, 180^\circ$ and 270° were selected to detail the process of amplitude and phase evolutions. Specifically, for the initial state of $\theta = 0^\circ$, the φ exhibits a precipitous decrease around 84.5 kHz and then levels off at off-resonance frequencies, the φ and $|\alpha|_r$ at resonance frequency reach $\varphi_r = 0^\circ$ and $|\alpha|_r = 51.72$ V/cm Oe, respectively, as illustrated in Fig. 2(b). As θ is increased to 90°, the φ_r of 180° and $|\alpha|_r$ of 28.64 V/cm Oe under resonance frequency were observed at resonance frequency. Evidently the resonance α exhibits 180° phase reversal with a modest decay in amplitude (as illustrated in Fig. 2(d)). Compared with the initial state of $\theta = 0^\circ$, the direction of applied H_{DC} reversed at $\theta = 180^\circ$. The $|\alpha|_r$ exhibits similar peak value of 51.93 V/cm Oe, while the φ_r appears 180° phase reversal as illustrated in Fig. 2(f). As θ is increased to 270°, the φ_r returns back to its initial state $\varphi_r = 0^\circ$, while the $|\alpha|_r$ of 27.08 V/cm Oe almost equals to that of $\theta = 90^\circ$ (As shown in Fig. 2(h)). To further understand this process, phase spectra around resonance in every adjacent θ states were extracted for comparison studies (as shown in Fig. 2(c), (e), (g), (i)). Distinct discrepancy in phase spectra can be observed, for $-90^\circ \leq \theta < 90^\circ$, $\varphi_r = 0^\circ$, while for $90^\circ \leq \theta < 270^\circ$, $\varphi_r = 180^\circ$. Namely, when θ is varied from -90° to 90° , the φ_r exhibits a similar “hold” state relative to its initial state; while the θ increase in the process of 90° – 270° , the φ shows a different “reverse” state relative to its prior state. Moreover, the phenomenon also occurred in the vicinity of the resonance frequency. In this case, the α can be expressed as

$$\alpha(\theta) = |\alpha| e^{-i\varphi}(\theta) = (|\alpha| \cos \varphi - i |\alpha| \sin \varphi)(\theta) = (\alpha' - i\alpha'')(\theta) \quad (1)$$

where $|\alpha|$ and φ are the amplitude and phase, α' and α'' are real and imaginary part of α , respectively. From experimental results we know that 180° phase reversal occurred at some key points, e.g., for $\theta = 90^\circ$, the $\varphi_r = 0^\circ$ and the $|\alpha|_r = 27.04$ V/cm Oe; for $\theta = 270^\circ$, the $\varphi_r = 180^\circ$ and $|\alpha|_r = 27.08$ V/cm Oe, exhibiting an undistorted 180° phase reversal of ME voltage coefficient at resonance triggered by magnetization direction reversal. More relative details for this process are required to explore from the aspect of complex quantity to follow.

Foregoing discussion mentioned that the ME voltage coefficient can

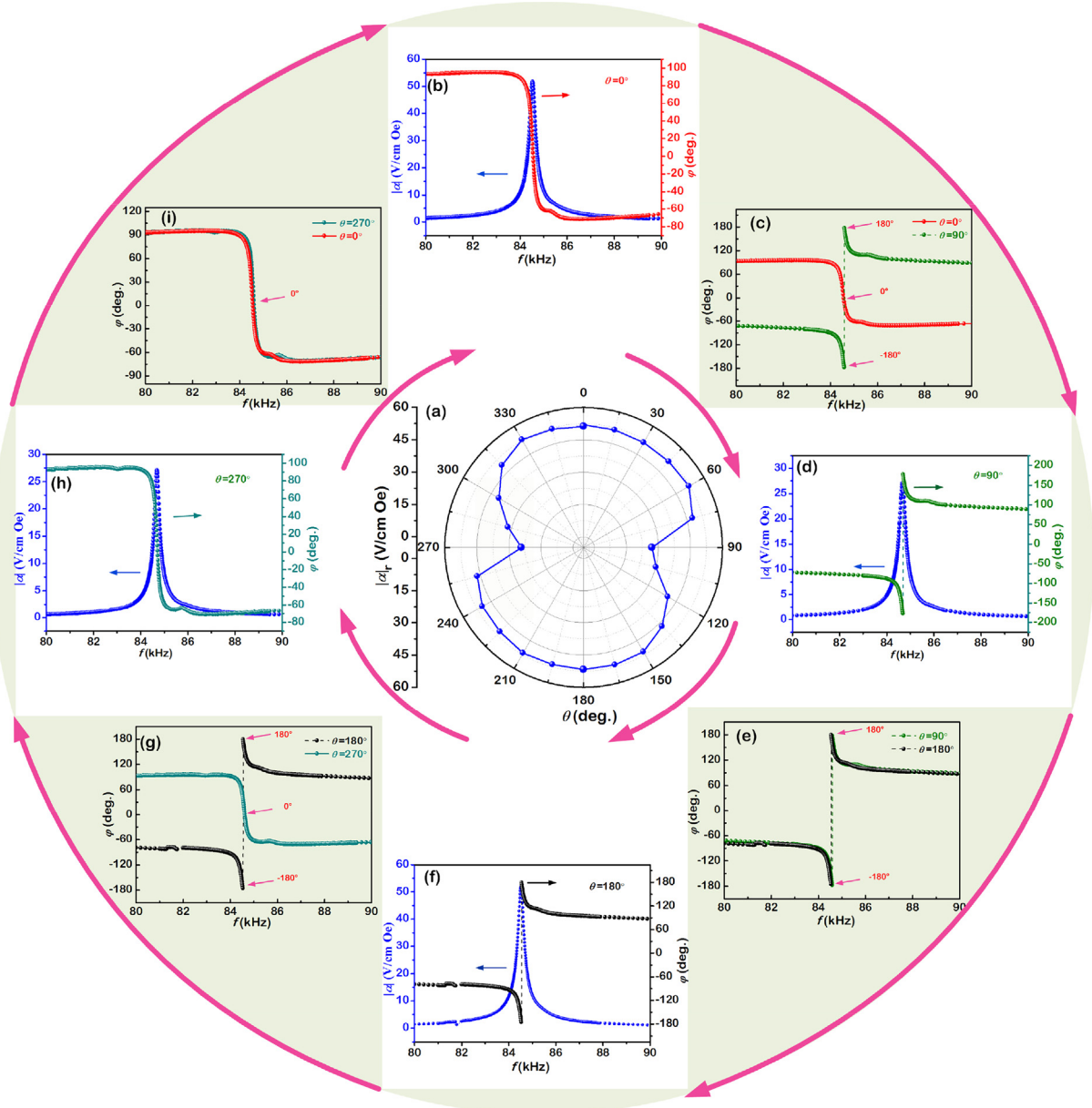


Fig. 2. (a) Representative $|\alpha|_r$ vs θ profile in polar coordinate plot with θ varied from 0° to 360° under optimum bias of 460e. Detailed amplitude and phase spectra in the range of 80–90 kHz for (b) $\theta = 0^\circ$, (d) $\theta = 90^\circ$, (f) $\theta = 180^\circ$ and (h) $\theta = 270^\circ$. Comparisons of φ vs f profiles for every two adjacent θ states, i.e., (c) $\theta = 0^\circ$ and 90° , (e) $\theta = 90^\circ$ and 180° , (g) $\theta = 180^\circ$ and 270° , (i) $\theta = 0^\circ$ and 90° .

be described as $\alpha = \alpha' - i\alpha''$ [20,33], wherein the real part of α' ($|\alpha|\cos\varphi$) was defined as strength of ME interactions displaying mutual energy exchange between magnetic and electric energy, while the imaginary part of α'' ($|\alpha|\sin\varphi$) was defined as mechanical loss of ME interactions in the dynamic magneto-mechanical-electric conversion process. In this regard, investigating the α' and α'' can further understand each variation tendency of phase angle and amplitude in ME coefficients. Fig. 3 depicted a comparison in α' and α'' for the representative cases of $\theta = 0^\circ$ and 180° , respectively. As shown in Fig. 3(a), for $\theta = 0^\circ$ the α' exhibits a significant positive peak value of +51.72 V/cm Oe at resonance frequency, and the α'' displays an increase to its maximum and then dramatic minimum successively around the resonance frequency. By contrast, for $\theta = 180^\circ$ the α' shows a negative peak of -51.93 V/cm Oe at resonance. Correspondingly, from the spectra we can see the α'' also undergoes a negative increase to minimum value then a maximum peak successively in vicinity of the resonance frequency. It is noteworthy that the complex quantity of α

swapped in sign but with its amplitude almost constant, e.g., for $\theta = 0^\circ$, the resonance ME voltage coefficient $\alpha = |\alpha|_r = 51.72$ V/cm Oe; while for $\theta = 180^\circ$, the resonance $\alpha = |\alpha|_r = -51.93$ V/cm Oe. The contrasting results were also shown in the Cole-Cole plots, as shown in Fig. 3(c). The Cole-Cole plot appears to be composed of two external tangent circles in the complex α plane with clockwise gradual frequency increasing, the radius of the circles is nearly identical, and the circles for $\theta = 0^\circ$ and 180° are symmetrically distributed right and left of the imaginary axis, respectively. Moreover, the circles of α' vs α'' demonstrate a reciprocal conversion between active power and reactive power and simultaneously accompanying a conversion of capacitive behavior to inductive behavior with frequency increasing or vice versa [27]. These results further demonstrate that once the magnetization direction is reversed, 180° phase reversal appears and amplitude retains constant in the vicinity of resonance frequency simultaneously. Therefore, the undistorted 180° phase reversal of ME response can be achieved in the vicinity of resonance by reversing the applied H_{DC}

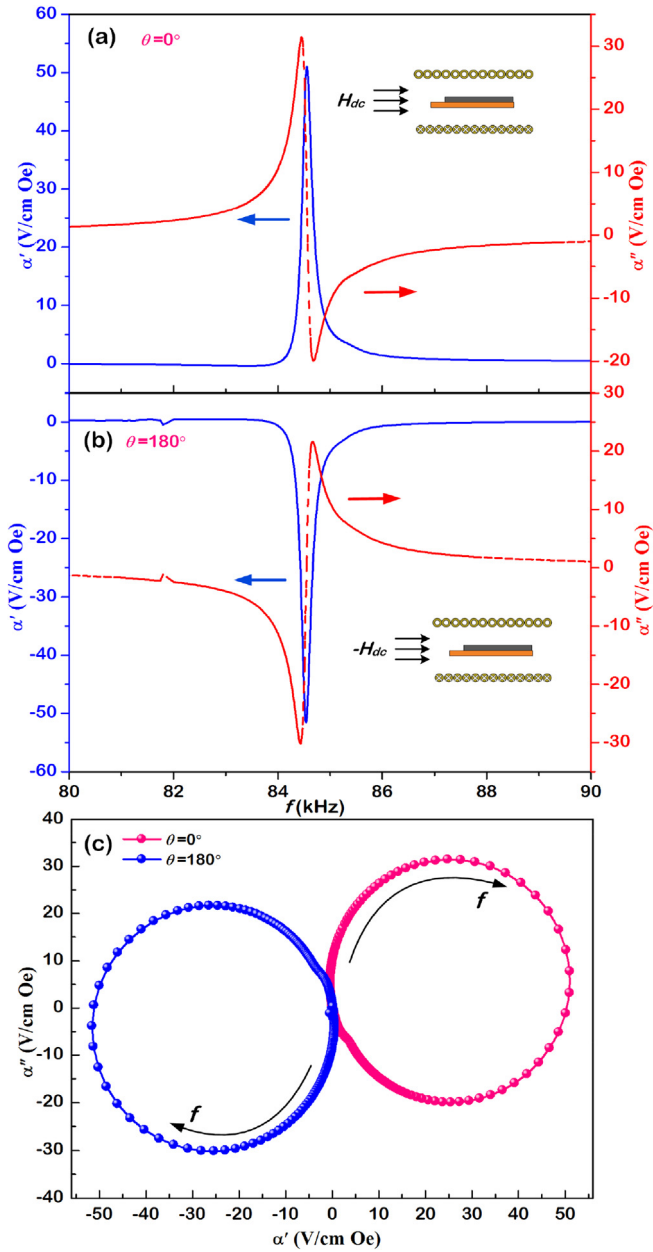


Fig. 3. Frequency dependence of α' and α'' for (a) $\theta = 0^\circ$ and (b) $\theta = 180^\circ$ in the range of 80–90 kHz. (c) Cole-Cole plots for $\theta = 0^\circ$ and 180° , and the arrow denotes the frequency increasing direction. Measurement was performed under optimum magnetic bias of $H_{DC} = 46$ Oe.

direction.

ME voltage coefficient can be roughly described as: $\alpha = kdg$, (k , d and g represent coupling factor, piezomagnetic coefficients and piezoelectric coefficients, respectively) [34]. Previous reports provided solid evidence that the magnetostrictive material exhibits distinct properties under applied H_{DC} with varied θ [35,36]. Therefore, as a function of θ , the α can be predicted as $\alpha(\theta) = k_c * g * d(\theta)$. In this regard, we can predict that the origins of 180° phase reversal with constant amplitude can be attributed to the dynamic piezomagnetic effect of magnetostrictive materials. To better understand the origin of 180° phase reversal with constant amplitude of the ME response, the dynamic piezomagnetic coefficient d ($d = d\lambda/dH_{AC}$) of the NZFO phase as a function of θ was investigated. A non-contact optical method is employed to characterize d , and the working principle for the measurements is in the following. Contractive velocity (v) of the end surface for the NZFO

phase along longitudinal direction is captured by a laser Doppler vibrometer and then monitored by a lock-in amplifier as a function of θ to calculate the complex contractive velocity, which can be obtained by multiplying a conversion factor of 10 mm/s/V. Then the displacement of Δl can be derived according to the driving frequency with the expression of $\Delta l = v/(2\pi f)$. Therefore, the dynamic piezomagnetic coefficient as a function of θ can be calculated from the expression of [37,38]

$$d(\theta) = 2\Delta l(\theta)/(lH_{AC}) \quad (2)$$

where $\Delta l(\theta)$ is the displacement at certain θ , l and H_{AC} are the length of sample and AC magnetic field, v is velocity, f is the driving frequency. Moreover, the d can be re-written and defined in the complex quantity form of

$$d = |d| e^{-i\varphi_2} = |d| \cos \varphi_2 - i |d| \sin \varphi_2 = d' - id'' \quad (3)$$

where $|d|$ is amplitude of dynamic piezomagnetic coefficient, φ_2 is the phase angle, d' and d'' are real part and imaginary of dynamic piezomagnetic coefficient, respectively. Fig. 4(a) shows the polar coordinate diagrams of $|d|$ at resonance frequency of 100.3 kHz under various θ and $H_{DC} = 46$ Oe. As θ is increased from 0° to 360° , similarly a twofold symmetry in the polar coordinate diagrams can be observed. Maximum and minimum resonance amplitudes of dynamic piezomagnetic coefficients $|d|_r$ of 23.3 ppm/Oe and 12.8 ppm/Oe were obtained at $\theta = 0^\circ$ (and 180°) and $\theta = 90^\circ$ (and 270°), respectively. For isotropic polycrystalline magnetostrictive materials, the magnetostriction λ as function of θ can be expressed as [39,40]

$$\lambda = \frac{3}{2}\lambda_s [\cos^2(\theta) - \frac{1}{3}] \quad (4)$$

where λ_s is the saturation magnetostriction, the $\cos(\theta)$ is the cosine of θ ($\theta = 0^\circ, 90^\circ, 180^\circ$ and 270°). Consider $d = d\lambda/dH_{AC}$, the $|d|$ as a function of θ can be given as

$$d = \frac{3}{2}d_s [\cos^2(\theta) - \frac{1}{3}] \quad (5)$$

where d_s is the saturation piezomagnetic coefficient. These results can be attributed to the variations in magnetization directions and demagnetization effects [32,41,42]. Fig. 4(b)–(i) illustrate representative φ_2 vs f curves and the corresponding comparisons in $\theta = 0^\circ, 90^\circ, 180^\circ$ and 270° . Similarly, the φ_2 appears in 180° phase reversal in the vicinity of resonance (as shown in Fig. 4(b) and (g)), but the φ_2 show a hold initial state for rotated H_{DC} direction (as shown in Fig. 4(c) and (e)). Specifically, for $-90^\circ \leq \theta < 90^\circ$, the φ_2 of 0° was observed at off-resonance frequency of $f_{off-r} = 100.6$ kHz, while the φ_2 of 60° was observed at resonance of $f_r = 100.3$ kHz; For $90^\circ \leq \theta < 270^\circ$, φ_2 was obtained at resonance with -120° , while φ_2 was obtained at off-resonance frequency of $f_{off} = 100.6$ kHz with 180° . This phenomenon arises from the relaxation of magneto-mechanical conversion in magnetostrictive material. These results demonstrate that reversed magnetization direction result in the 180° phase reversal with constant amplitude of dynamic piezomagnetic coefficient at resonance frequency. The dynamic piezomagnetic coefficient d vs θ profile essentially tracks the ME voltage coefficient α vs θ profile as expected. Therefore, solid evidence demonstrate that changed H_{DC} direction induced the 180° phase reversal with constant amplitude of dynamic piezomagnetic coefficient, resulting in the undistorted 180° phase reversal of the ME response.

Similarly, two representative comparison data for $\theta = 0^\circ$ and 180° were also selected to show more details about the dynamic piezomagnetic coefficient in the form of complex quantity. For $\theta = 0^\circ$, d' and d'' spectra in the range of 95–105 kHz were plotted in Fig. 5(a). Real part of d' undergoes a relaxation process in the vicinity of resonance frequency with its maximum positive peak of 15.84 ppm/Oe, and imaginary part d'' exhibits a significant positive peak of 22.24 ppm/Oe. By contrast, at $\theta = 180^\circ$, the d' and d'' swapped in sign as illustrated in

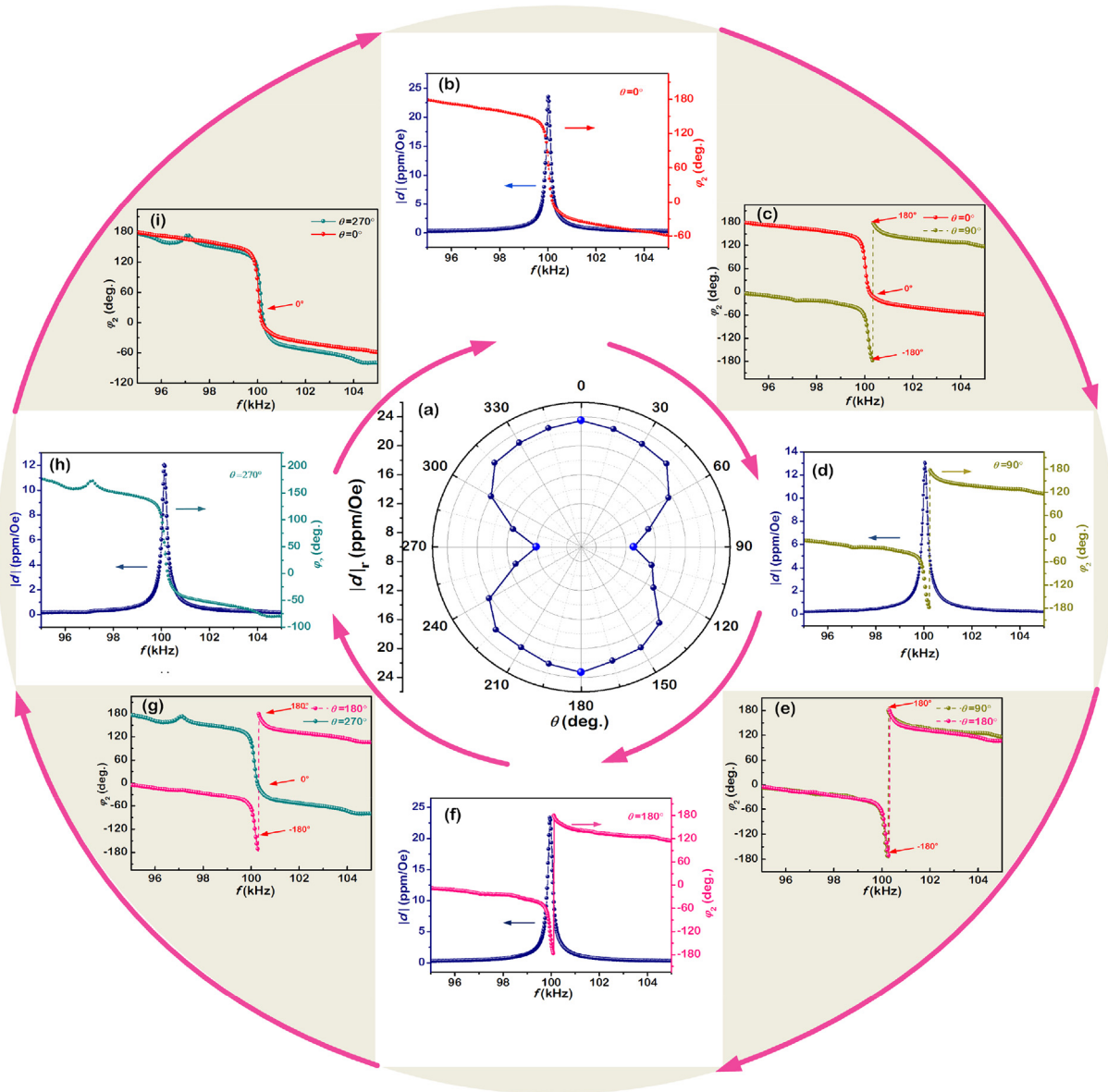


Fig. 4. (a) Representative $|d|_r$ vs θ profile in polar coordinate plot with θ varied from 0° to 360° under optimum bias of 46Oe. Detailed amplitude and phase spectra in the range of 80–90 kHz for (b) $\theta = 0^\circ$, (d) $\theta = 90^\circ$, (f) $\theta = 180^\circ$ and (h) $\theta = 270^\circ$. Comparisons of φ vs f profiles for every two adjacent θ states, i.e., (c) $\theta = 0^\circ$ and 90° , (e) $\theta = 90^\circ$ and 180° , (g) $\theta = 180^\circ$ and 270° , (i) $\theta = 0^\circ$ and 90° .

Fig. 5(b), exhibiting a mirror image along real axis due to the reversal of θ . Similarly the corresponding Cole-Cole plots were shown in Fig. 5(c) for comparison, d' vs d'' with frequency increasing from 95 kHz, the circles with identical radius for $\theta = 0^\circ$ and 180° occupy opposite positions in the plot, exhibiting φ_2 appears 180° reversal and $|d|$ retains in the frequency of 95–107 kHz. Furthermore, the Cole-Cole plot exhibits a typical relation of storage modulus and losses of eddy current and relaxation in magnetostrictive material. These results further demonstrate that the 180° phase reversal with constant amplitude of dynamic piezomagnetic coefficient was induced by the reversed magnetization direction. Experiments demonstrate that the H_{DC} direction control of dynamic piezomagnetic coefficient is in compliance with that of the ME response. Therefore, we conclude that the undistorted 180° phase reversal in the ME response can be achieved by reversed H_{DC} direction, which is mainly attributed to the symmetrical nature of the dynamic piezomagnetic coefficient vs H_{DC} curve (y-axis symmetric nature of the magnetostriction vs H_{DC} curve) in the magnetostrictive layer.

4. Conclusion

In summary, 180° phase reversal with constant amplitude of ME output in PZT-8/NZFO laminate was realized by rotating the applied field, and the dynamic piezomagnetic effect can account for its origins. The result shows that the undistorted 180° phase reversal in ME response can be achieved by taking advantage of the reversed DC field direction to change magnetization direction of NZFO plate. At the specific cases of $\theta = 0^\circ$ and $\theta = 180^\circ$, equal amplitude but swapped in sign for the ME voltage coefficients of $+51.72$ V/cm Oe and -51.93 V/cm were obtained and more explicit view was given in Cole-Cole plots. Undistorted 180° phase reversal can provide great potentials in 180° ME phase shifters and inverters.

Acknowledgments

This research was financially supported by National Natural Science Foundation of China (NSFC) (Grant No. 61973279), Key Scientific Research Projects for Universities in Henan Province (Grant No.

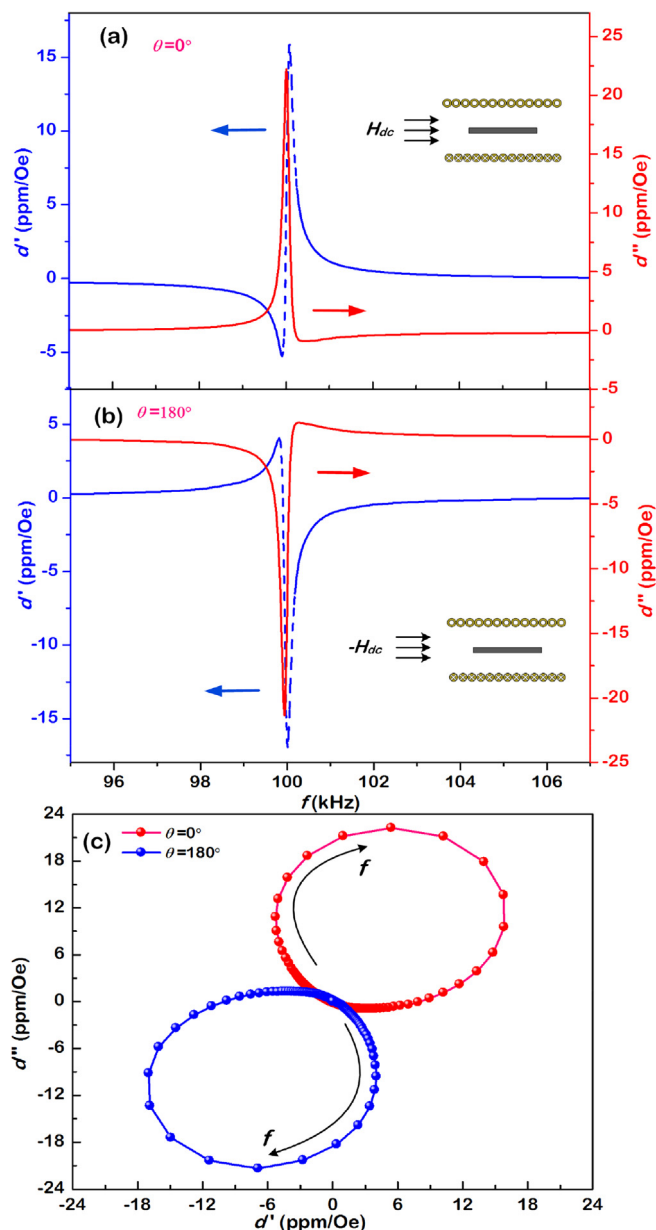


Fig. 5. Frequency dependence of d' and d'' for (a) $\theta = 0^\circ$ and (b) $\theta = 180^\circ$ in the range of 95–107 kHz. (c) Cole-Cole plots for $\theta = 0^\circ$ and 180° , and the arrow denotes the frequency increasing direction. Measurement was performed under optimum magnetic bias of $H_{DC} = 46$ Oe.

18A535001). The study at Russia was supported by the Russian Foundation for Basic Research (Grant No. 18-52-00021). The research at Oakland University was supported by a grant from the National Science Foundation (Grant No. DMR-1808892).

References

[1] N.A. Spaldin, R. Ramesh, Nat. Mater. 18 (2019) 203.

[2] A.A. Amirov, V.V. Rodionov, V. Komanicky, V. Latyshev, E.Y. Kaniukov, V.V. Rodionova, J. Magn. Magn. Mater. 479 (2019) 287.
 [3] A. Lasheras, J. Gutierrez, J. Magn. Magn. Mater. 479 (2019) 282.
 [4] J.T. Zhang, W.W. Zhu, D.A. Filippov, W. He, D.Y. Chen, K. Li, S.T. Geng, Q.F. Zhang, L.Y. Jiang, L.Z. Cao, R. Timilsina, G. Srinivasan, Rev. Sci. Instrum. 90 (2019) 015004.
 [5] Z. Li, W.Z. Qi, J. Cao, Y. Li, G. Viola, C.L. Jia, H.X. Yan, J. Alloy Compd. 788 (2019) 701.
 [6] C.M. Leung, J.F. Li, D. Viehland, X. Zhuang, J. Phys. D: Appl. Phys. 51 (2018) 263002.
 [7] P.B. Meisenheimer, S. Novakov, N.M. Vu, J.T. Heron, J. Appl. Phys. 123 (2018) 240910.
 [8] L.Y. Fetisov, D.V. Chashin, D.D. Plekhanova, D.V. Saveliev, Y.K. Fetisov, J. Magn. Magn. Mater. 470 (2019) 93.
 [9] J.T. Zhang, W.W. Zhu, D.Y. Chen, K. Li, Q.F. Zhang, X.L. Wang, X.W. Zheng, L.Y. Jiang, L.Z. Cao, Eur. Phys. J. Appl. Phys. 85 (2019) 20601.
 [10] A. Banerjee, J.T. Zhang, P. Zhou, K. Tuppil, G. Sreenivasulu, H.W. Qu, T.J. Zhang, R. Timilsina, F.A. Chavez, G. Srinivasan, J. Magn. Magn. Mater. 460 (2018) 424.
 [11] T.X. Nan, J.M. Hu, M.Y. Dai, S. Emori, X.J. Wang, Z.Q. Hu, A. Matyushov, L.Q. Chen, N.A. Sun, Adv. Funct. Mater. 29 (2019) 1806371.
 [12] X. Xue, G.H. Dong, Z.Y. Zhou, D. Xiang, Z.Q. Hu, W. Ren, Z.G. Ye, W. Chen, Z.D. Jiang, M. Liu, ACS Appl. Mater. Int. 9 (2017) 43188.
 [13] M. Sarathbavan, K. Annamalai, T. Parida, K.R. Kumar, A.M. Strydom, K. Ramamurthi, K.K. Bharathi, J. Magn. Magn. Mater. 474 (2019) 144.
 [14] I.V. Golosovsky, A.K. Ovsyanikov, D.N. Aristov, P.G. Matveeva, A.A. Mukhin, M. Boehm, L.P. Regnault, L.N. Bezmaternykh, J. Magn. Magn. Mater. 451 (2018) 443.
 [15] J.T. Zhang, W.W. Zhu, D.Y. Chen, H.W. Qu, P. Zhou, M. Popov, L.Y. Jiang, L.Z. Cao, G. Srinivasan, J. Magn. Magn. Mater. 473 (2019) 131.
 [16] S.X. Dong, J.F. Li, D. Viehland, J. Appl. Phys. 95 (2004) 2625.
 [17] Z.Q. Chu, M. PourhosseiniAsl, S.X. Dong, J. Phys. D: Appl. Phys. 51 (2018) 243001.
 [18] M.I. Bichurin, V.M. Petrov, S.V. Averkina, E. Liverts, J. Appl. Phys. 107 (2010) 053904.
 [19] J.Y. Zhai, J.F. Li, D. Viehland, M.I. Bichurin, J. Appl. Phys. 101 (2007) 014102.
 [20] J.V. Vidal, A.V. Turutin, I.V. Kubasov, M.D. Malinkovich, Y.N. Parkhomenko, S.P. Kobleeva, A.L. Kholkin, N.A. Sobolev, IEEE Trans Ultrason. Ferr. 64 (2017) 1102.
 [21] Z.Q. Chu, V. Annapureddy, M. PourhosseiniAsl, H. Palneedi, J. Ryu, S.X. Dong, MRS Bull. 43 (2018) 199.
 [22] J.T. Zhang, D.Y. Chen, D.A. Filippov, K. Li, Q.F. Zhang, L.Y. Jiang, W.W. Zhu, L.Z. Cao, G. Srinivasan, Appl. Phys. Lett. 113 (2018) 113502.
 [23] J.T. Zhang, D.Y. Chen, K. Li, D.A. Filippov, B.F. Ge, Q.F. Zhang, X.X. Hang, L.Z. Cao, G. Srinivasan, AIP Adv. 9 (2019) 035137.
 [24] A. Stupakov, A. Perevertov, J. Magn. Magn. Mater. 456 (2018) 390.
 [25] X.W. Dong, Y.J. Wu, J.G. Wan, T. Wei, Z.H. Zhang, S. Chen, H. Yu, J.M. Liu, J. Phys. D: Appl. Phys. 41 (2008) 035003.
 [26] J.T. Zhang, W. He, M. Zhang, H.M. Zhao, Q. Yang, S.T. Guo, X.L. Wang, X.W. Zheng, L.Z. Cao, Rev. Sci. Instrum. 86 (2015) 095005.
 [27] Z. Shi, L.Z. Chen, Y.S. Tong, H. Xue, S.Y. Yang, C.P. Wang, X.J. Liu, Appl. Phys. Lett. 102 (2013) 112904.
 [28] Z. Shi, L.Z. Chen, Y.S. Tong, Z.B. Zheng, S.Y. Yang, C.P. Wang, X.J. Liu, Acta. Phys. Sin. 62 (2013) 017501.
 [29] Y. Yang, Y.J. Ma, J.P. Zhou, G.B. Zhang, J.H. Peng, IEEE Trans Magn. 52 (2016) 1000404.
 [30] M.J. PourhosseiniAsl, Z.Q. Chu, X.Y. Gao, S.X. Dong, Appl. Phys. Lett. 113 (2018) 092902.
 [31] Z.X. Chen, Y. Su, S.A. Meguid, J. Appl. Phys. 116 (2014) 173910.
 [32] X.X. Cui, S.X. Dong, J. Appl. Phys. 109 (2011) 083903.
 [33] D.R. Patil, Y. Chai, R.C. Kambale, B.G. Jeon, K. Yoo, J. Ryu, W.H. Yoon, D.S. Park, D.Y. Jeong, S.G. Lee, J. Lee, J.H. Nam, J.H. Cho, B.I. Kim, K.H. Kim, Appl. Phys. Lett. 102 (2013) 062909.
 [34] C.W. Nan, Prog. Mater. Sci. 37 (1993) 1.
 [35] H. Wang, Z.D. Zhang, R.Q. Wu, L.Z. Sun, Acta Mater. 61 (2013) 2919.
 [36] S.M. Na, J.J. Park, S. Lee, S.Y. Jeong, A.B. Flatau, Mater. Lett. 213 (2018) 326.
 [37] J.T. Zhang, P. Li, Y.M. Wen, W. He, A.C. Yang, C.J. Lu, Appl. Phys. Lett. 103 (2013) 202902.
 [38] J.T. Zhang, P. Li, Y.M. Wen, W. He, A.C. Yang, C.J. Lu, Sens. Actuat. A: Phys. 214 (2014) 149.
 [39] C.B. Jiang, H.B. Zhang, Z.B. Wang, H.B. Xu, J. Phys. D: Appl. Phys. 41 (2008) 155012.
 [40] Y.M. Pei, D.N. Fang, Smart Mater. Struct. 17 (2008) 065001.
 [41] C.S. Zhang, T.Y. Ma, M. Yan, J. Appl. Phys. 110 (2011) 063901.
 [42] Y.M. Pei, X. Feng, X. Gao, D.N. Fang, J. Alloy. Compd. 476 (2009) 556.